

## ANTENNA ARRAY PATTERN SYNTHESIS AND WIDE NULL CONTROL USING ENHANCED PARTICLE SWARM OPTIMIZATION

M. A. Mangoud and H. M. Elragal

Department of Electrical and Electronics Engineering  
University of Bahrain  
P. O. Box 32038, Isa Town, Kingdom of Bahrian

**Abstract**—In this paper, Enhanced Practical Swarm Optimization (EPSO) algorithm is proposed to be applied to pattern synthesis of linear arrays. Updating formulas of global best particle position and velocity are modified to improve the convergence accuracy of classical Practical Swarm Optimization. The developed EPSO is tested and compared with a standard benchmark to be validated as an efficient optimization tool for beamforming applications. Different numerical examples are presented to illustrate the capability of EPSO for pattern synthesis with a prescribed wide nulls locations and depths. Collective multiple deep nulls approach and direct weights perturbations approach are considered to obtain adaptive wide null steering subject to peak side lobe level and minimum main beam width constraints. Starting from initial Chebyshev pattern, single or multiple wide nulls are achieved by optimum perturbations of elements current amplitude or complex weights to have either symmetric or asymmetric nulls about the main beam. Proper formation of the cost function is presented for all case studies as a key factor to include the pattern constraints in the optimization process.

### 1. INTRODUCTION

Beamforming techniques that allow the placement of single or multiple nulls in the antenna pattern at specific interference directions have been extensively studied in the literature. Prescribed nulls in the radiation pattern need to be formed to suppress interferences from specific directions [1]. For broadband interference, nulls in the pattern

---

Corresponding author: M. A. Mangoud (mangoud@eng.uob.bh).

should be wide and deep enough to suppress peak side lobe levels (SLL) at the angular sector of arrival of the interference. Wide nulls are formed in conventional techniques by placing multiple adjacent nulls in the radiation pattern [1] or by using evolutionary optimization techniques [2]. The nulling methods are generally based on controlling the complex weights (amplitude and the phase control) [3, 4], the amplitude only [5, 6], the phase-only [7, 8], and the position only of the array elements [9, 10]. Interference suppression with complex weights is the most efficient because it has greater degrees of freedom for the solution space. In this paper, special attention will be given to optimize element coefficients that possess even symmetry about the center of linear array as the number of attenuators/phase shifters and the computational time are halved.

As the wide null steering is a highly nonlinear optimization problem, evolutionary optimization algorithms are proved to be a capable method of obtaining best solutions for this kind of applications. Evolutionary optimizations, such as the genetic algorithm [2, 7], ant colony optimization [3, 10], differential evolution [11], particle swarm optimization (PSO) [12], are used extensively to optimize and perturb array parameters for null steering and pattern synthesis purposes. PSO in particular shows superior solutions compared to conventional analytical approaches, classical optimizations and other evolutionary optimizations techniques. Previous trials to improve the performance of the standard PSO have been reported in the literature [13–15].

In this paper, a modified version of PSO with enhanced searching ability is introduced. New terms are added to the global best position and the velocity updating equations. The new terms are based on fitness to distance ratio of swarm particles; as will be shown this method proves to give better results for global minimum. Subsequently, the proposed enhanced version of PSO (EPSO) is applied to solve the problem of synthesis antenna array patterns. The remainder of the paper is organized as follows. A general overview of the classical PSO scheme and proposed EPSO technique is introduced in Section 2. Section 3 explains formulation of the pattern synthesis problem and the wide nulling for linear antenna array. The cost function that is used in the minimax optimization process for the control of the wide null and synthesis the pattern shape is presented. In Section 4, the numerical examples are provided to show the capability of EPSO, and numerical results are discussed. Finally, the conclusion is made in Section 5.

## 2. ENHANCED PARTICLE SWARM OPTIMIZATION (EPSO)

Particle Swarm Optimization is a swarm intelligence method for global optimization. Each individual, named particle, of the population, called *swarm*, adjusts its trajectory toward its own previous best position and toward the previous best position attained by any member of its topological neighborhood. The basic PSO algorithm consists of three steps:

1. The positions  $x^i(k)$  and velocities  $v^i(k)$  of the initial population of particles are randomly generated for the  $i$ th particle at time  $k$ . Where  $i$  is the current particle number in the swarm;  $i \in \{1, 2, \dots, S\}$  and  $S$  is the swarm size.
2. Update velocities of all particles at time  $k + 1$  as follows:

$$v^i(k+1) = w \cdot v^i(k) + c_1 \cdot r_1 \cdot (p^i(k) - x^i(k)) + c_2 \cdot r_2 \cdot (p^g(k) - x^i(k)) \quad (1)$$

where,  $r_1$  and  $r_2$  are uniformly distributed random variables in  $[0, 1]$  range. The fitness function values determines which particle has the best position value  $p^i(k)$  over the current swarm and also updates the global best position  $p^g(k)$  for the current and all the previous swarm moves. The three terms in the equation represent the current motion, particle own memory, and swarm influence. These parameters are summed with three weights, namely, inertia factor,  $w$ , self confidence factor,  $c_1$ , and swarm confidence factor,  $c_2$ , respectively. Velocity updates here are influenced by both the best global solution and the best local solution in the current population.

3. The position of each particle is updated using its velocity vector at time  $k + 1$  as:

$$x^i(k+1) = x^i(k) + v^i(k+1) \quad (2)$$

The three steps of velocity update, position update, and fitness calculations are repeated until a desired convergence criterion is met. Two modifications are proposed to enhance the performance of classical PSO. Firstly, updating global best particle position with zero velocity according to the following equation:

$$p^g(k+1) = [1 + \lambda \cdot U]p^g(k) \quad (3)$$

where  $U$  is chose to be a Gaussian random number with zero mean and unit variance, and  $\lambda$  is a convergence acceleration parameter that represents the weighting of stochastic acceleration term that pulls

each particle towards global best location. Adding randomness to the position of the global best location may lead to better value for global best solution. This is proposed for classical PSO; some global best particle solution could be trapped far away from other particles solutions in the swarm. Secondly, two new terms in the velocity updating Equation (1) are introduced as follows:

$$v^i(k+1) = w \cdot v^i(k) + c_1 \cdot r_1 \cdot (p^i(k) - x^i(k)) + c_2 \cdot r_2 \cdot (p^g(k) - x^i(k)) \\ + c_3 \cdot r_3 \cdot (p_{fdr}^i(k) - x^i(k)) + c_4 \cdot r_4 \cdot (p_{fdr}^g(k) - x^i(k)) \quad (4)$$

where,  $c_3$  and  $c_4$  are acceleration constants;  $r_3$  and  $r_4$  are uniformly distributed random variables in  $[0, 1]$  range.  $p_{fdr}^i(k)$  and  $p_{fdr}^g(k)$  are two new local and global candidate positions that are selected by locating the individual with minimum fitness to distance ratio (FDR) over all particles in the swarm. The local and global FDR for each particle at time  $k$  are defined as:

$$\text{FDR}_{\text{local}}^i = \frac{\text{fitness}(p^g(k)) - \text{fitness}(x^i(k))}{\text{dist}(p^i(k), x^i(k))} \quad (5)$$

$$\text{FDR}_{\text{global}}^i = \frac{\text{fitness}(p^g(k)) - \text{fitness}(x^i(k))}{\text{dist}(p^g(k), x^i(k))} \quad (6)$$

where  $\text{fitness}(\cdot)$  is the cost function to be minimized, and  $\text{dist}(p^g(k), x^i(k))$  is a measure related to the distance between the particle's global best position and all other particles on the swarm, which is defined as

$$\text{dist}(p^g(k), x^i(k)) = \left| \sum_{n=1}^N \sqrt{p_n^z(k)^2 - x_n^i(k)^2} \right| \quad (7)$$

where  $p^z(k)$  is either the local best  $p^i(k)$  or global best  $p^g(k)$  position vector;  $p_n^z(k)$  is the  $n$ th components of the global best vector.  $x_n^i(k)$  is the  $n$ th components of the  $i$ th particle position vector  $x^i(k)$  which is represented as  $x^i(k) = (x_1^i, x_2^i, \dots, x_N^i)$  in the  $N$ -dimensional search space (particle size).

The added two terms in the proposed velocity updating Equation (4) are influenced by the FDR measures which ensure the selection of the candidate with fitness function value that is close enough to global best solution. At the same time, the selected candidate has a far enough distance from global and local best positions as shown in (5) and (6). This way shows better perturbation for individual particles in the swarm and leads to better search for global minimum as will be shown in Section 4.

### 3. OBJECTIVE FUNCTION FOR WIDE NULL CONTROL OF LINEAR ANTENNA ARRAY

Adaptive wide nulling for broad-band interference suppression is achieved by perturbing the current weights of array elements. Simultaneously, it is always desirable to keep the main beam width (directivity) and the peak SLL within a certain given level. This is realized by solving minmax optimization problem that is subject to three constrains for SLL limits, the prescribed depth of the wide null and main beam acceptable broadening. The problem can be described as:

$$\begin{aligned} \min_{I_n} \in c \{ \max_{\theta_{\min} \leq \theta \leq \theta_{\max}} |\text{AF}(I_n, \theta, d_n)| \} \\ \text{s.t. } \text{MSL}_1 \leq \text{SLL} \& \text{MSL}_2 \leq \text{wide null depth} \& \Delta\text{BW} \leq \delta \end{aligned} \quad (8)$$

where  $\text{AF}(I_n, \theta, d)$  is the array factor as a function of current coefficients ( $I_n$ ), the angle with respect to the direction of the antenna array ( $\theta$ ) and distance between elements ( $d_n$ ).  $\theta_{\min}$  and  $\theta_{\max}$  are the elevation angles' minimum and maximum boundaries for the prescribed wide null. *s.t.* is subject to constraint;  $C$  is the set of all vectors with complex components. The complex vector  $I_n$  is the optimization parameter. SLL is the pattern peak side lobe level;  $\text{MSL}_1$  is the prescribed value for SLL excluding the main beam band;  $\text{MSL}_2$  is the peak SLL in the region of wide null;  $\Delta\text{BW}$  and  $\delta$  are the change and the maximum allowable change in the main beam width respectively. Linear antenna array of  $2N$  isotropic elements is considered in this paper. The array is positioned symmetrically along the  $z$  axis, and the array factor for this structure can be expressed as

$$\text{AF}(\psi) = \sum_{n=-N}^N I_n e^{j d_n \psi} \quad (9)$$

where  $I_n = I_n^{\text{Re}} + j \cdot I_n^{\text{Im}}$ , ( $n = -N, \dots, -2, -1, 1, 2, \dots, N$ ) are the complex excitations of each element in the array,  $\psi = k \cdot \sin(\theta)$  and  $k$  is the wave number. Therefore, the real and imaginary parts of the array factor are

$$\text{Re}\{\text{AF}(\psi)\} = \sum_{n=-N}^N I_n^{\text{Re}} \cos(d_n \psi) - I_n^{\text{Im}} \sin(d_n \psi) \quad (10)$$

$$\text{Im}\{\text{AF}(\psi)\} = \sum_{n=-N}^N I_n^{\text{Im}} \cos(d_n \psi) - I_n^{\text{Re}} \sin(d_n \psi) \quad (11)$$

Two cases are considered for the current coefficients of the array elements. **Case 1 (amplitude only control):**  $I_{-n}^{\text{Re}} = I_n^{\text{Re}}$ , the excitation coefficients are real and symmetrical around the center of the array; this case gives symmetrical pattern about the main beam direction ( $\theta_m = 0$ ). Since  $I_n^{\text{Im}} = 0$  and  $\sin(-d_n\psi) = -\sin(d_n\psi)$ , the imaginary part of AF in (11) equals 0. While, the real array factor (10) is reduced as following

$$\text{AF}(\psi) = 2 \sum_{n=1}^N I_n^{\text{Re}} \cdot \cos(d_n\psi) \quad (12)$$

**Case 2 (full amplitude/phase control):**  $I_{-n} = I_n^*$  the excitation coefficients are complex and conjugate symmetrical around the center of the array; this means that  $I_{-n}^{\text{Re}} = I_n^{\text{Re}}$  and  $I_{-n}^{\text{Im}} = -I_n^{\text{Im}}$ ; this case gives anti-symmetrical pattern about the main beam direction ( $\theta_m = 0$ ). In this case, also the imaginary part of (11) equals 0, and the real array factor (10) can be written as

$$\text{AF}(\psi) = 2 \sum_{n=1}^N I_n^{\text{Re}} \cdot \cos(d_n k \psi) - I_n^{\text{Im}} \cdot \sin(d_n k \psi) \quad (13)$$

It is well known that the Chebyshev current distribution gives the optimum pattern in terms of the sidelobe level and the main beam width for equally spaced arrays. Starting from initial array factor pattern of Chebyshev array  $\text{AF}_i(\psi)$ , the current coefficients ( $I_n$ ) are optimized to steer the wide null and achieve the required synthesized pattern according to (8). Inspired by the cost function implemented previously in [5], a novel best objective function is developed as following:

$$\text{Fitness} = \sum_{\theta=-\frac{\pi}{2}}^{\theta=\frac{\pi}{2}} (|W_{\text{null}}(\theta) \cdot \text{AF}_i(\psi) - \text{AF}_i(\psi)|)^2 + C(\theta) \quad (14)$$

where  $\text{AF}_i(\psi)$  is the initial Chebyshev radiation pattern;  $W_{\text{null}}(\theta)$  is the weighting function that specifies the wide nulls locations. The objective function is built by adding two terms. The first term is the summation (over all sample points) of the squared value for the difference between the desired and the initial array factors. The second term is a function that related to the SLL and the depth of the null constraints.  $C(\theta)$  is selected so that each constraint is weighted by a coefficient to emphasize its relative importance. A computer program has been developed to optimize (14) with array factors presented in (9)–(13) for the two cases of amplitude only and complex coefficients control using EPSO, and the results is discussed next.

### 4. NUMERICAL RESULTS

The capabilities of the proposed EPSO technique for synthesis of the radiation pattern of a linear array will be presented in this section. Before undertaking the paper’s main synthesis problem, a validation test for EPSO algorithm is performed. A canonical problem of  $N$  elements linear array composed of isotropic elements with broadside ( $\theta_m = 90$ ) is optimized in [16], and it is published to be used as a benchmark that gives the global optimum array placement and weighting. Optimum current weights and separation distances of array elements are obtained using ESPO to minimize peak SLL and compared with the results presented in [16] for  $N = 6$  two case studies that are proved to be global minimum solutions. As shown in Fig. 1, the Magnitude of Array Factor obtained using the developed EPSO coincides well with benchmark array factor patterns [16]. For a given beam width ( $BW = 30^\circ$ ) case, the obtained peak SLL is  $-24.2$  dB, and for a given ( $BW = 60^\circ$ ) case, peak SLL =  $-51.2$  dB is obtained. These values are exactly the same as the results presented in [16].

For the purpose of wide null pattern synthesis, deterministic method known as collective multiple deep nulls approach [2] is applied. Nulls are imposed to the pattern with amplitude only control. Starting with a given initial pattern  $AF_i(\psi)$  with a given main beam and side lobe envelop. The corresponding coefficients  $\{I_{no}\}$  that produce this initial pattern are then perturbed such that the resultant pattern would have nulls at the desired direction ( $\psi_m$ ) according to the following

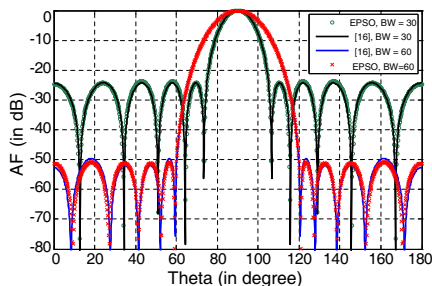


**Figure 1.** Comparison between the developed EPSO tool and Balanis benchmark [1], Magnitude of Array Factor for optimal array for  $N = 6$  elements, (a)  $BW = 30^\circ$ ,  $\theta_d = 90^\circ$ , (b)  $BW = 60^\circ$ ,  $\theta_d = 90^\circ$ .

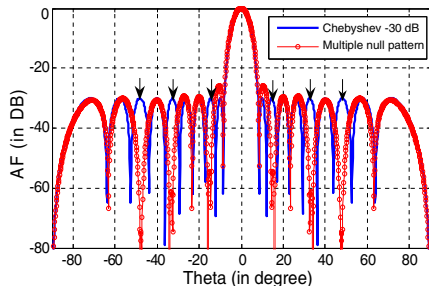


**Figure 2.** Initial and perturbed (optimized) 30 dB Chebyshev pattern ( $N = 10$  elements) with three symmetrical nulls imposed at  $\theta = 14.49^\circ$ ,  $32.65^\circ$  and  $48.06^\circ$  using collective multiple deep nulls approach.

formula:

$$I_n = I_{\text{no}} - \sum_{n=1}^M \gamma_m \cdot e^{jd_n k \psi_m} \quad (15)$$

where  $M$  is the number of nulls needed to be imposed to the original pattern, and  $\gamma_m$  are constants that are obtained using PSO. For all subsequent numerical examples the optimization process will be initiated with a classic Chebyshev design of 20-element linear array  $\lambda/2$  inter-element spacing and SLL envelop not to exceed  $-30$  dB.

Figure 2 shows the initial and perturbed (optimized) patterns using collective multiple deep nulls approach with three prescribed nulls imposed at  $\theta_m = 14.49^\circ$ ,  $32.65^\circ$  and  $48.06^\circ$ . It should be noted that symmetric nulls is observed at  $-\theta_m$  locations since Case 1 (amplitude only control) with AF described in (12) is considered here. The corresponding nulls are reduced to about  $-80$  dB while the SLL of the perturbed pattern is maintained at  $-30$  dB except the first lobe that becomes  $-26.5$  dB, and the main beam width is almost unchanged compared to the initial pattern.

Next, the problem of antenna pattern synthesis described in (8) is investigated. The objective will be to synthesize a pattern that has a broad null located at  $35^\circ$  with  $\Delta\theta_i = 30^\circ$  with optimum peak side lobe level and maximum directivity. The optimum target design will be subject to the constraint that in the wide null region it is desired to depress the SLL to less than  $-50$  dB i.e., null depth  $-20$  dB relative to the side peak SLL. Also, we constrain the peak SLL to not exceed  $-30$  dB. Also, constraining the percentage of loss in directivity (main beam widening) to a minimum value is an objective. The desired pattern is achieved using firstly, the method of collective multiple deep nulls (Fig. 3) then secondly, using EPSO (Figs. 4–6) to emphasize its potential and capability for wide nulling and pattern synthesis.

Results of applying collective multiple deep nulls approach to form a prescribed wide null are illustrated in Fig. 3. As shown five nulls are imposed to realize the suppressed sector from  $20^\circ$  to  $50^\circ$ . The SLL at the target sector is found to be relatively high null depth (between **-35 dB** and  $-66$  dB) while the pattern peak SLL becomes  $-26$  dB. Having more deep SLL in the target sector region, number of imposed nulls needs to be increased. However, this may lead to uncontrolled values for the pattern peak SLL.

Continuing on the preceding synthesis example, the EPSO algorithm presented in Section 2 is applied to impose the same wide null with the objective of having more control on the peak SLL and getting minimum null depth values using the cost function (14). Fig. 4 depicts initial and optimized radiation patterns with the prescribed wide null in the band  $[20^\circ, 50^\circ]$ . EPSO algorithm is implemented to optimize the objective function (14) without the use of the term  $C(\theta)$  which means



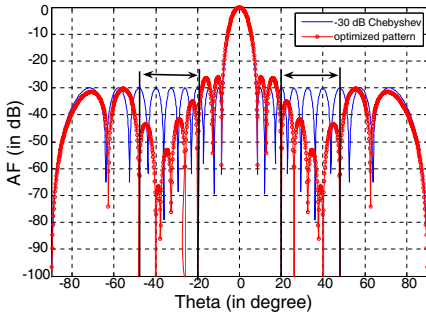


**Figure 3.** Original and perturbed (optimized) with symmetrical wide null imposed by 5 nulls at  $\theta = 20^\circ$  to  $50^\circ$ .

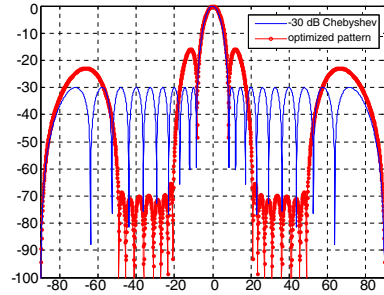


**Figure 4.** Perturbed (unconstrained optimized)  $-30$  dB Chebyshev pattern ( $N = 20$  elements) main beam steered at  $0^\circ$  with symmetrical wide null imposed at  $\theta = 20^\circ$  to  $50^\circ$  but peak SLL  $> -30$ .

no constraint on the peak SLL is applied. Amplitude only control (12) is used here; therefore, a symmetric image wide null on the pattern is observed at the sector  $[-20^\circ, -50^\circ]$ . The algorithm uses the following parameters: swarm size = 20, number of generations = 100000, inertia weight factor  $w = 0.5$ , acceleration constants  $c_1 = 2$ ,  $c_2 = 2$ ,  $c_3 = 0.5$ ,  $c_4 = 0.5$ . The dynamic range allowed for elements amplitude perturbation  $(\Delta I_n) \in \{-1.5, 1.5\}$ . As seen in Fig. 4, A perfect wide null ( $-67$  dB) in the target sector is achieved, and at the same time the main beam width is unchanged. However, peak SLL becomes  $-20$  dB at the two close-in lobes next to the main beam.

$$W_{\text{null}}(\theta) = \begin{cases} 100 & \text{if } \theta_1 \leq \theta \leq \theta_2 \text{ (wide null region)} \\ 50 & \text{otherwise} \end{cases} \quad (16)$$

To allow a full control of the peak SLL to be  $\leq -30$  dB and to have wide-band null at the exact placement simultaneously, the following term  $C(\theta)$  is added to the cost function as in (14).

$$C(\theta) = \begin{cases} 5 & \text{if } \text{MSL}_1 \leq -30 \text{ or } \text{MSL}_2 \leq -50 \\ 0 & \text{otherwise} \end{cases}, \quad (17)$$

Figure 5 shows the initial pattern and two optimized patterns. As can be seen the  $\text{PSLL} \leq -30$  dB is obtained successfully. However, as expected it is found that as the wide null becomes deeper, more broadening in the main beam width (BW) occurs. Maximum allowable

tolerance in the main beam broadening is controlled in the EPSO implementation by the definition of band range of  $MSL_1$  used in (17). The initial Chebyshev AF has beam width of  $16^\circ$  centered about  $0^\circ$  at  $-30$  dB. By allowing the beam width at  $-30$  dB to become ( $BW = 18^\circ, 19^\circ$  and  $20^\circ$ ), we achieved wide null depths of ( $MSL_2 = -50, -52$  and  $-67$  dB) respectively. The two patterns with deep nulls at **-50 dB and -67 dB** are illustrated in Fig. 5.

To achieve non symmetrical null in the pattern with a deeper null values, the synthesis of the elements with perturbing complex weights (full amplitude and phase control case) as described in (13) is applied. Assume initial array coefficients denoted as  $(I_{no}^{Re} + jI_{no}^{Im})$  for the initial pattern. Besides changing the real part of roots to get the wide null,  $\Delta I_n^{Re} \in \{-1.5, 1.5\}$ ., small perturbations of the imaginary parts  $\Delta I_n^{Im} \in \{-0.15, 0.15\}$  were found also to be necessary in order to maintain the rest of the pattern side lobes under strict control. As shown in Fig. 6. The pattern is non-symmetric about the main beam, as null is imposed at only the positive band  $[20^\circ, 50^\circ]$ . Maximum deep null is achieved in this case with the value of **-70 dB** with  $BW = 20^\circ$ . The numerical results for previous EPSO implementations (Figs. 3–6) that were performed are shown in Table 1. The table lists real/ complex current excitations for the 20 elements of the initial and optimized arrays. The main beam width for each case is presented in the first row, and the wide null band depth ( $MSL_2$ ) and the peak SLL values

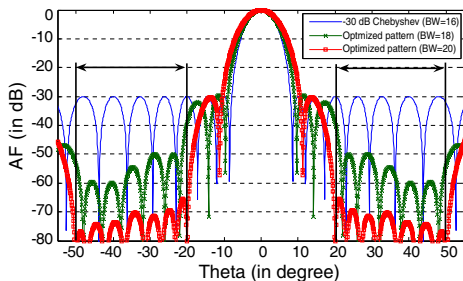


**Figure 5.** Two different perturbed (optimized) with  $BW = 18^\circ$  and  $20^\circ$  and Chebyshev pattern  $BW = 16^\circ$ , ( $N = 20$  elements) and symmetrical wide null imposed at  $\theta = 20^\circ$  to  $50^\circ$ ,  $SLL = -30$  dB.

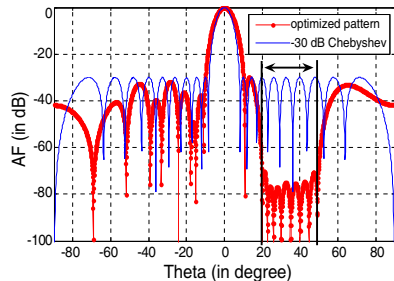


**Figure 6.** Original and perturbed (optimized)  $-30$  dB Chebyshev pattern ( $N = 20$  elements) with non-symmetrical wide null imposed at  $\theta = 20^\circ$  to  $50^\circ$ .

**Table 1.** Currents of array elements for the initial Chebyshev pattern and the optimized pattern to impose wide null at  $[20^\circ, 50^\circ]$  with null depth, peak SLL and mainbeam width for different cases.

$k$	Initial chebyshev pattern	Perturbed pattern (amplitude only) MNM, Fig.3	Perturbed pattern (amplitude only) EPSO, Fig.4	Perturbed pattern (amplitude only) EPSO, Fig.5			Perturbed pattern (complex current) EPSO, Fig.6
	BW=16°	BW=16°	BW=16°	BW=18°	BW=19°	BW=20°	BW=20°
$\pm 1$	4.8116	4.9208	5.0900	5.3070	5.4365	6.2905	6.7978 $\mp$ 0.1486i
$\pm 2$	4.6677	4.6143	5.4687	5.1075	5.3548	6.1638	6.5920 $\pm$ 0.1486i
$\pm 3$	4.3902	4.4148	5.0476	4.5588	4.7164	5.4365	5.7374 $\pm$ 0.0725i
$\pm 4$	3.9986	3.8150	5.4980	4.2159	4.4154	4.9786	4.8471 $\pm$ 0.1430i
$\pm 5$	3.5195	3.4841	4.1962	3.4458	3.3072	3.6969	3.6969 $\mp$ 0.0436i
$\pm 6$	2.9848	3.0849	3.9408	3.0911	2.8000	2.9858	2.8415 $\mp$ 0.0338i
$\pm 7$	2.4280	2.4398	2.2183	2.1373	1.6531	1.7028	1.8583 $\pm$ 0.0513i
$\pm 8$	1.8815	2.2993	1.6624	1.6918	1.1790	1.1319	1.1112 $\pm$ 0.0436i
$\pm 9$	1.3741	1.1468	0.5479	0.7832	0.4432	0.3969	0.6122 $\pm$ 0.1444i
$\pm 10$	1.5667	0.8082	0.3038	0.4374	0.2313	0.1960	0.1261 $\pm$ 0.1500i
MSL <sub>1</sub>	-30	-35	-67	-50	-52	-65	-70
MSL <sub>2</sub>	-30	-28	-20	-30	-30	-30	-30

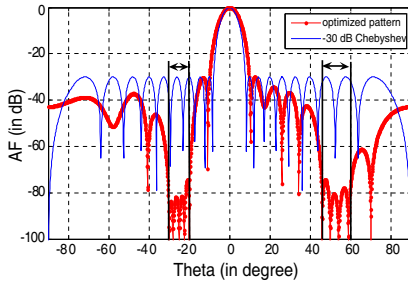
(MSL<sub>1</sub>) are included in the last two rows.

Final example is presented to get more insight into the capability of EPSO to synthesize the pattern with multiple non symmetrical wide nulls while maintaining the peak SLL bounded to a given constraint value. Multiple wide nulls with minimum SLL at the bands  $[-30^\circ, -20^\circ]$  and  $[45^\circ, 60^\circ]$  are assumed to be imposed in the desired pattern. For these assumptions, EPSO algorithm optimize the fitness function in (14) with weighting function adopted as follows

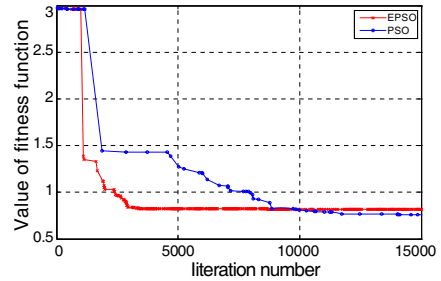
$$W_{\text{null}}(\theta) = \begin{cases} 100 & \text{if } -30^\circ \leq \theta \leq -20^\circ \text{ (wide null 1 region)} \\ 100 & \text{if } 45^\circ \leq \theta \leq 60^\circ \text{ (wide null 2 region)} \\ 50 & \text{otherwise} \end{cases} \quad (18)$$

Figure 8 shows the accurately produced prescribed wide nulls with null depth = -73 dB (with BW allowed to 20° at -30 dB) for Region 1 and Region 2 with complex weights control as in (13). The constraint having peak SLL less than -30 dB is included in the  $C(\theta)$  term in the objective function (14).

Figure 7 shows the convergence of EPSO fitness values compared with classical PSO for the case study in Fig. 6. History of fitness values for the first 15000 swarm generations is illustrated for both classical PSO and EPSO implementations. As can be seen classical PSO has faster convergence than EPSO algorithm. However, EPSO reaches lower values than the minimum that is obtained with PSO. The previous numerical results obtained in this section show the superiority of EPSO as an efficient tool for beamforming wide null and synthesis of the pattern to have peak side lobe level fixed at a certain level



**Figure 7.** Perturbed (optimized) 30 dB Chebyshev pattern ( $N = 20$  elements) main beam steered at  $0^\circ$  with two wide nulls imposed at  $\theta_1 = -30^\circ$  to  $-20^\circ$  and  $\theta_2 = 45^\circ$  to  $60^\circ$ .



**Figure 8.** Comparison of classical and enhanced PSO schemes with the convergence test for to achieve the target wide null between  $[20^\circ, 50^\circ]$ .

with minimum changes in the main beam width (directivity). This is performed by different perturbing techniques of amplitude or complex weights of the current of array elements. Also, it is demonstrated how to properly select the weighting function used in the objective function (14) for different examples as it is the key factor for this type of optimization problems.

## 5. CONCLUSION

An efficient enhanced version of particle swarm optimization algorithm is presented for the purpose of suppressed SLL of wide region in the pattern while preserving the peak side lobe level and main beam width at prescribed values. The global search ability of available PSO has been enhanced by adopting some modification to its updating formulas. The robust EPSO algorithm was successfully applied for wide null steering while preserving PSLL and BW, and this is proved by some numerical examples. Without increase in the dimensions of the array, EPSO algorithm enables the design of the linear array pattern with accurate wide null steering and minimum null depth. In each of the presented examples EPSO algorithm easily achieved the optimization goal. By comparing with PSO, EPSO demonstrates superiority in achieving optimum end result value and higher convergence accuracy.

## REFERENCES

1. Steyskal, H., R. A. Shore, and R. L. Haupt, "Methods for null control and their effects on the radiation pattern," *IEEE Transactions on Antennas and Propagation*, Vol. 34, 404–409, 1986.
2. Lu, Y. and B. K. Yeo, "Adaptive wide null steering for digital beamforming array with the complex coded genetic algorithm," *IEEE Int. Conf. Phased Array Systems and Technology*, 557–560, Dana Point CA, USA, 2000.
3. Karaboga, D., K. Guney, and A. Akdagli, "Antenna array pattern nulling by controlling both the amplitude and the phase using modified touring ant colony optimisation algorithm," *Int. Journal of Electronics*, Vol. 91, 241–251, 2004.
4. Guney, K. and A. Akdagli, "Null steering of linear antenna arrays using a modified tabu search algorithm," *Progress In Electromagnetics Research*, PIER 33, 167–182, 2001.
5. Guney, K. and M. Onay, "Amplitude-only pattern nulling of linear antenna arrays with the use of bees algorithm," *Progress In Electromagnetics Research*, PIER 70, 21–36, 2007.
6. Babayigit, B., A. Akdagli, and K. Guney, "A clonal selection algorithm for null synthesizing of linear antenna arrays by amplitude control," *Journal of electromagnetic Waves and Applications*, Vol. 20, No. 8, 1007–1020, 2006.
7. Haupt, R. L., "Phase-only adaptive nulling with a genetic algorithm," *IEEE Transactions on Antennas and Propagation*, Vol. 45, 1009–1015, 1997.
8. Mouhamadou, M., P. Armand, P. Vaudon, and M. Rammal, "Interference supression of the linear antenna arrays controlled by phase with use of SQP algorithm," *Progress In Electromagnetics Research*, PIER 59, 251–265, 2006.
9. Ismail, T. H. and M. M. Dawoud, "Null steering in phased arrays by controlling the element positions," *IEEE Transactions on Antennas and Propagation*, Vol. 39, 1561–1566, 1991.
10. Akdagli, A., K. Guney, and D. Karaboga, "Pattern nulling of linear antenna arrays by controlling only the element positions with the use of improved touring ant colony optimization algorithm," *Journal of Electromagnetic Waves and Applications*, Vol. 16, No. 10, 1423–1441, 2002.
11. Yang, S. W., Y. B. Gan, and A. Y. Qing, "Antenna-array pattern nulling using a differential evolution algorithm," *Int. Journal of RF and Microwave Computer Aided Eng.*, Vol. 14, 57–63, 2004.

12. Khodier, M. M. and C. G. Christodoulou, "Linear array geometry synthesis with minimum sidelobe level and null control using particle swarm optimization," *IEEE Transactions on Antennas and Propagation*, Vol. 53, 2674–2679, 2005.
13. Ho, S. L., S. Yang, G. Ni, et al., "A particle swarm optimization method with enhanced global search ability for design optimizations of electromagnetic devices," *IEEE Transactions on Antennas and Propagation*, Vol. 42, 1107–1110, 2006.
14. Schutte, J. F. and A. A. Groenword, "A study of global optimization using particle swarms," *Journal of Global Optimiz.*, Vol. 31, 93–108, 2005.
15. Li, W.-T., X.-W. Shi, and Y.-Q. Hei, "An improved particle swarm optimization algorithm for pattern synthesis of phased arrays," *Progress In Electromagnetics Research*, PIER 82, 319–332, 2008.
16. Bevelacqua, P. J. and C. A. Balanis, "Minimum sidelobe levels for linear arrays," *IEEE Transactions on Antennas and Propagation*, Vol. 55, No. 12, 3442–3449, Dec. 2007.

**Errata to ANTENNA ARRAY PATTERN SYNTHESIS  
AND WIDE NULL CONTROL USING ENHANCED  
PARTICLE SWARM OPTIMIZATION** by M. A.-A. Mangoud  
and H. M. Elragal, in *Progress In Electromagnetics Research B*, Vol. 17,  
1–14, 2009

1) In Fig. 8 legend PSO and EPSO are reversed and the curves should be as follows:

PSO (x — red) and EPSO ( o — blue)

2) Replace the word Figure 7 by Figure 8 (and vice versa) in page 11.